Biophysical Journal, Volume *112*

Supplemental Information

Effects of Polymer Length and Salt Concentration on the Transport of ssDNA in Nanofluidic Channels

Weixin Qian, Kentaro Doi, and Satoyuki Kawano

Langevin dynamics simulation of a coarse-grained ssDNA model

In our model, intramolecular interactions are represented by a linear spring, and the electrokinetics of polymer molecules are mainly affected by external electric fields in liquids. In such a case, the behavior of particles can be expressed by an over-damped Langevin equation (1–3):

$$\xi(\mathbf{v}_i - \mathbf{u}) = -\nabla U_i + \mathbf{R}_i + q(\mathbf{E} - \nabla\phi), \tag{S1}$$

where $\mathbf{v}_i$ is the velocity of the ith particle, $\mathbf{E} = E_z\mathbf{e}_z$ where E_z is the electric field strength and $\mathbf{e}_z$ is the unit vector in the z-direction, ξ is the friction coefficient of particle, $\mathbf{u}$ is the EOF velocity field that is treated as a field fixed in the space for the polymer translocation such that $\mathbf{u}(r) = u_z(r)\mathbf{e}_z$, $-\nabla U_i$ is the conservative force including interactions between particles, q is the electrical charge of single particle, and $\mathbf{R}_i$ denotes the random force that satisfies the fluctuation-dissipation theorem:

$$\begin{cases} \langle R_{vi}(t)\rangle = 0 \\ \langle R_{vi}(t)\cdot R_{vj}(t')\rangle = 2k_BT\xi\delta_{ij}\delta(t-t'), \quad v = \{x, y, z\} \end{cases} \tag{S2}$$

where k_B is the Boltzmann constant, T is temperature, δ_{ij} is Kronecker's delta, and $\delta(t–t')$ is the Dirac delta function where t and t' are time. The polymer chain consists of N individual particles bonded to neighbors with a linear spring (1–3). Interactions between the nearest neighbors and between the coarse-grained molecule and channel surface are represented by the Lennard-Jones potential taking the volume exclusion effect into account (1–3):

$$U_{\mathrm{LJ}}(\mathbf{r}_i) = \begin{cases} \sum_{\substack{j=1 \\ j\neq i}}^{N} 4\varepsilon_{\mathrm{LJ}}\left[\left(\frac{\sigma}{r_{ij}}\right)^{12} - \left(\frac{\sigma}{r_{ij}}\right)^{6}\right] + \varepsilon_{\mathrm{LJ}} & \text{for } r_{ij} \le 2^{\frac{1}{6}}\sigma \\ 0 & \text{for } r_{ij} > 2^{\frac{1}{6}}\sigma \end{cases} \tag{S3}$$

where r_{ij} is the distance between the two molecules, σ is the diameter, and $\varepsilon_{\mathrm{LJ}}$ is the energy well-depth set to k_BT. The coarse-grained molecule corresponds to 12 nucleotides (nt), which is determined by dividing the persistence length of 5.0 nm for ssDNA by 0.43 nm associated with the interval between nucleotides, holding the internal structure and properties of ssDNA (4). U_{LJ} was applied to non-adjacent molecules. For the purposes of volume exclusion, the potential was truncated at $r = \sqrt[6]{2}\sigma$ to allow for purely repulsive interactions between the molecules. The repulsive force from the channel surface works only on the surface normal direction. Bonding between two consecutive molecules along the chain is given by (1–3)

$$U_{bond}(\mathbf{r}_i) = \begin{cases} \frac{1}{2}\sum_j k(r_{ij} - r_{eq})^2 & \text{for neighbors} \\ 0 & \text{otherwise} \end{cases} \tag{S4}$$

where r_{eq} is the equilibrium distance between the connected molecules and given by 5.0 nm. The spring constant is written by $k = k_BT/\delta$, and δ is caused by thermal fluctuations around the average

and $\delta = 0.1\sigma$ is applied (1–3). The other parameter set employed in the present simulations was already published (1). The friction coefficient ξ and effective bead charge q in Eq. S1 are evaluated referring to experimental data of diffusion coefficient D and electrophoretic mobility μ of ssDNA (5). In this study, we set $T = 300$ K and $\varepsilon = 80.1$ for aqueous solutions. Resulting from the relationship of $\xi = k_B T/ND$ and $q = \xi\mu = \mu k_B T/ND$ (5), both ξ and q are described as a function of N.

At the beginning of LD simulations, a polymer structure equilibrated in free solution is placed at the cylindrical nanochannel inlet apart from the distance of R_g and forced to pass into the channel by applying a uniform electric field of $E_z = 1.0 \times 10^5$ V/m. Linear increase in the electrophoretic velocity to applied electric fields is also confirmed for the case of $E_z = 1.0 \times 10^6$ V/m. That is, the mobility is constant for each N. Based on this fact, we discuss the electrophoretic characteristics of ssDNA for the actual magnitude of the electric field. Entering the polymer into the nanochannel, its structure deforms and reaches a steady state during translocation in the cylindrical channel. This preliminary computation is carried out for each trial to determine the initial condition in the nanochannel. Based on previous studies (1–3), the time step of LD simulation is set to 1.0 ps, and the total computational time is 2.0 ms for each. The time step of 1.0 ps is constrained by both stability and accuracy, which was already verified in a previous study (1). The analysis of the polymer transport is evaluated by at least 20 individual trials in all cases with different surface charges and ion concentrations.

Verification of the coarse-grained ssDNA model

The polymer transport properties, i.e., D, μ, and R_g, were evaluated by performing the LD simulation in free solution as shown in Fig. S1. D was determined from the Einstein relation calculating mean square displacements of the ssDNA and μ was directory analyzed from the simulations applying uniform electric fields to obtain the terminal velocity as a function of the electric field. R_g was determined as $R_g^{\,2} = \sum_{i=1}^{N} \left(\mathbf{r}_i - \mathbf{r}_c\right)^2 / (N+1)$, where $\mathbf{r}_c$ is the center of mass of the chain. More details were also in a previous study (1). Our simulation results were in close agreement with the theoretical evaluations of D and μ. This means that the coarse-graining method is suitable to represent the behavior of ssDNA in terms of diffusion and electrophoresis. Setting q and ξ for a single bead to reproduce the D and μ, R_g of the ssDNA consequently agreed with the theoretical model as shown in Fig. S1(c). As listed in Table 2 in the main text, appropriately determined q and ξ for a coarse-grained molecule resulted in the constant mobility of 3.0×10^{-8} m^2/Vs equivalent among each polymer length. These parameters for a coarse-grained molecule are suitable to define a building block of ssDNA. Thus, this model is valid to mimic various lengths of ssDNA, corresponding to from 60 to 600 nt.

In the simulation, the electric field in the nanochannel is assumed to be not altered by the presence of ssDNA. The charge density of ssDNA is calculated by:

$$\rho = Nq \Big/ \left(\frac{4}{3}\pi N r^3 \right) = \frac{3q}{4\pi r^3} \tag{S5}$$

where N is the number of beads, q is the electrical charge of a bead, and r is the bead radius. The electrical charge density is defined by dividing the total charge of a polymer by the volume. The ρ of the ssDNA chain and for comparison, that of the monovalent electrolyte solution with the concentration of C are listed in Table S1 in the unit of elementary charge per cubic nanometer. It is found that for C = 1, 2×10^{-2}, 4×10^{-3}, 9×10^{-4}, and 4×10^{-4} M, the charge density of ssDNA bead is at least one order of magnitude larger or smaller than that of the electrolyte solution, except in the case of $C = 2 \times 10^{-2}$ M. Thus, it is preferably assumed that the electrical charge of ssDNA is sufficiently screened and the presence of the DNA does not disturb the electric field in the nanochannel.

Table S1. Charge densities, ρ, of the electrolyte solution with C and ssDNA with the length N.

C (M)	ρ (e/nm^3)	N	ρ (e/nm^3)
1	6×10^{-1}	5	3×10^{-2}
2×10^{-2}	1×10^{-2}	10	3×10^{-2}
4×10^{-3}	2×10^{-3}	20	2×10^{-2}
9×10^{-4}	5×10^{-4}	30	1×10^{-2}
4×10^{-4}	2×10^{-4}	50	1×10^{-2}

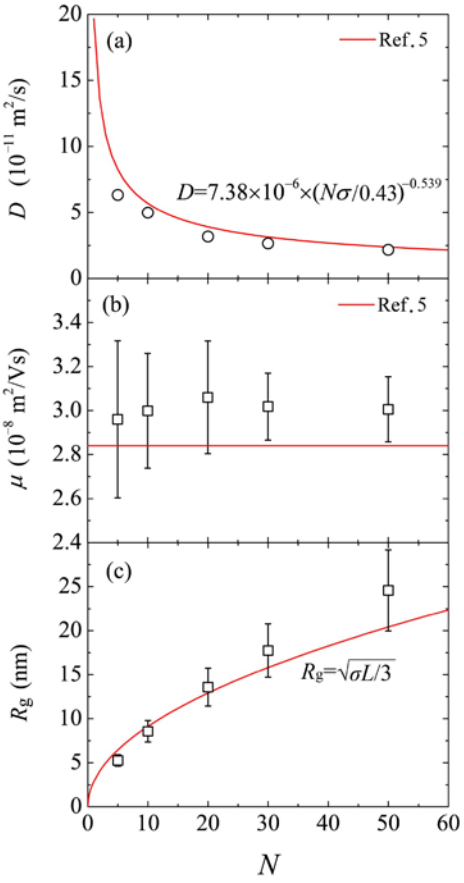

FIGURE S1. (a) Diffusion coefficient, D, (b) electrophoretic mobility, μ, and (c) radius of gyration, R_g, as a function of the polymer length of coarse-grained ssDNA, N. Error bars mean standard deviations at each data point. In (a), each data point was evaluated from the mean square displacement and the Einstein relation, averaged by 50 individual simulations in free solution. In (b), the displacement of the center of mass of the ssDNA chain was evaluated in the electric field of E_z = 1.0 × 10^5 V/m as a result of 60 trials, where the mobility of the coarse-grained ssDNA, $\mu = q/\xi$, was evaluated as 3.0 × 10^{-8} m^2/Vs that was constant for each N as shown in Table 2 in the main text. In (c), each data point results from 2000 data samples. σ and L are the persistence length and contour length of polymer, respectively, where we applied σ = 5 nm and $L = N\sigma$ for ssDNA.

Non-constant viscosity model

Taking into account the effect of velocity gradients due to highly concentrated ions near wall surfaces, the nanochannel is divided into two parts with respect to the radius r, such as the constant viscosity layer (CVL) in $0 \le r < b$, where the viscosity $\eta(r)$ is equal to the bulk value η_0, and the nonconstant viscosity layer (NVL) in $b \le r \le a$, where a is the radius of cylindrical channel and b is the boundary at the CVL and NVL. The viscosity expressed by $\eta(r) = \eta_0 r^2/b^2$ quadratically increases very near the channel surface as suggested by Wang et al. (6). Under an axially applied electric field E_z along the nanochannel, charged molecules and liquids are forced to migrate along the z-axis. Additionally, the ζ potential of a channel surface causes to form an EDL and a non-uniform electric field E_r along the r-axis, such that $E_r = -\mathrm{d}\phi/\mathrm{d}r$. Based on previous theoretical studies (1,7), an electric field is independently separated into two components, such as E_z and E_r. Here, we assume E_z is axially constant in the infinitely long narrow channel. Additionally, the pressure gradient along the z-axis is assumed to be negligibly small according to the conventional models of EOF (8). The EOF velocity $u_z(r)$ varied along the radial direction can be written in the cylindrical coordinate system as follows:

$$\frac{1}{r}\frac{\mathrm{d}}{\mathrm{d}r}\left(r\eta(r)\frac{\mathrm{d}u_z}{\mathrm{d}r}\right) = \varepsilon_0\varepsilon E_z \frac{1}{r}\frac{\mathrm{d}}{\mathrm{d}r}\left(r\frac{\mathrm{d}\phi}{\mathrm{d}r}\right), \tag{S6}$$

where ε_0 is the dielectric constant of vacuum and ε the relative dielectric constant of solution. The electric force on the right-hand side is derived from the Poisson equation. The electric potential $\phi(r)$ in the nanochannel is written by Eqs. 2 and 3 in the main text. Since the electric potential in nanochannel depends only on r, $\nabla^2\phi$ can be reduced to an ordinary differential equation and results in

$$\frac{\mathrm{d}u_z}{\mathrm{d}r} = \frac{\varepsilon_0\varepsilon E_z}{\eta(r)}\frac{\mathrm{d}\phi}{\mathrm{d}r}, \tag{S7}$$

The concrete solution of Eq. S7 can be expressed according to the boundary conditions. In the CVL, the solution of Eq. S7 is expressed replacing $\eta(r)$ by the constant viscosity η_0. The solution is represented in the form as follows:

$$u_z = \frac{\varepsilon_0\varepsilon E_z\zeta}{\eta_0}\left[\frac{I_0(\kappa r)}{I_0(\kappa a)} + C_1\right] \quad \text{in } 0 \le r < b, \tag{S8}$$

where C_1 is an integral constant determined later. On the other hand, in the NVL applying $\eta(r)$ presented above (6), Eq. 5 is expressed as follows

$$u_z = \frac{\varepsilon_0\varepsilon E_z\zeta b^2}{\eta_0 I_0(\kappa a)}\int\frac{\kappa I_1(\kappa r)}{r^2}\mathrm{d}r \quad \text{in } b \le r \le a. \tag{S9}$$

To solve Eq. S9, Meijer G function is introduced (9). The integral of the first order modified Bessel

function divided by r^2 is calculated as

$$\int \frac{\kappa I_1(\kappa r)}{r^2} \mathrm{d}r = -\frac{\kappa^2}{4} G_{1,3}^{2,0}\left(\begin{matrix} 1 \\ 0,0,-1 \end{matrix} \middle| -\frac{\kappa^2 r^2}{4} \right) + C_2 , \tag{S10}$$

and thus, the solution can be simplified, such that

$$u_z = -\alpha G(\kappa r) + C_2 , \tag{S11}$$

where $G(\kappa r) = G_{1,3}^{2,0}\left(\begin{matrix} 1 \\ 0,0,-1 \end{matrix} \middle| -\frac{\kappa^2 r^2}{4} \right)$ calculated by using Matlab® libraries and α is an EOF velocity parameter $\alpha = \varepsilon_0 \varepsilon E_z \zeta \kappa^2 b^2 / (4\eta_0 I_0(\kappa a))$. Based on the noslip boundary condition $u_z|_{r=a} = 0$, C_2 is determined and the solution results in

$$u_z = \alpha \left[G(\kappa a) - G(\kappa r) \right]. \tag{S12}$$

The velocity profile is continuous at $r = b$, such that

$$u_z(r \to b_{+0}) = u_z(r \to b_{-0}), \tag{S13}$$

that leads to C_1 as follows:

$$C_1 = I_0(\kappa b) + \frac{4}{\kappa^2 b^2} \left[G(\kappa a) - G(\kappa b) \right]. \tag{S14}$$

Sorting out the equations above, the solution of EOF velocity profile in the whole nanochannel results in

$$u_z(r) = \begin{cases} \alpha \left[\frac{4}{\kappa^2 b^2} \left(I_0(\kappa r) - I_0(\kappa b) \right) + G(\kappa a) - G(\kappa b) \right], & r \in [0, b) \\ \alpha \left[G(\kappa a) - G(\kappa r) \right], & r \in [b, a] \end{cases} \tag{S15}$$

EOF velocity profile with non-constant viscosity layer

Herein, the channel surface is positively or negatively polarized, controlling the ζ potential that is applied between −25 and 25 mV. Following a suggestion by Zhang et al. (10) that the thickness of NVL was set to 2 nm corresponding to the thickness of 5 atomic layers, the radius of CVL was set to b = 13 nm in an a = 15 nm radius of cylindrical channel. In the CVL, the bulk viscosity η_0 of water was set to 0.893 × 10^{-3} Pa·s. A uniform electric field of E_z = 1.0 × 10^5 V/m was applied along the z-direction. Figures S2 shows a difference between constant and non-constant viscosities in the EOF velocity field. When we set λ_D = 5 nm and NVL thickness (a − b) to 2 nm, the velocity in the non-constant viscosity liquid averagely decreased about 10% compared to the constant viscosity flow. It is found that as assumed in the model, the high viscosity near the wall surface due to highly concentrated solvent molecules cause to suppress ion transport and decrease EOF velocity to some extent. The EOF velocity profile for various λ_D, which was set to 0.3, 2, 5, 10, and 15 nm, corresponding to the ion concentration of 1, 2 × 10^{-2}, 4 × 10^{-3}, 9 × 10^{-4}, and 4 × 10^{-4} M, respectively,

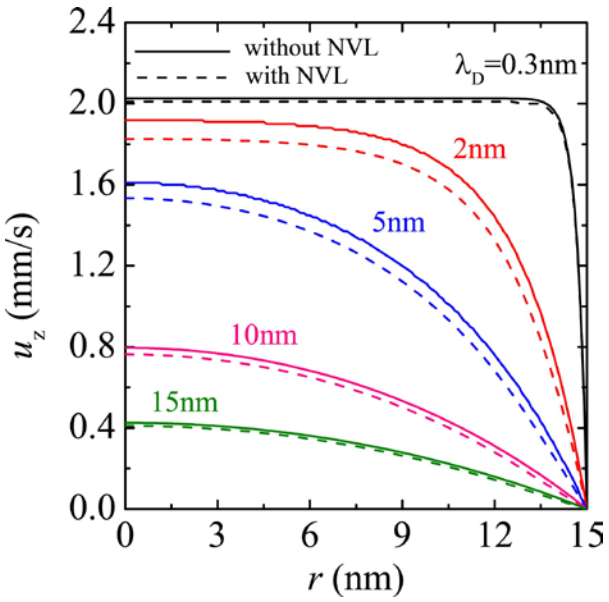

FIGURE S2. Comparison of EOF velocity profiles between with (dashed lines) and without (solid lines) the nonconstant viscosity layer for the case of λ_D = 5 nm, ζ = 25 mV, and NVL thickness of 2 nm (b = 13 nm).

as shown in Table 1 in the main text. Transition in the flow profile from Poiseuille-like flow to plug-like one was clearly found with decreasing λ_D, corresponding to increase in the ion concentration. The velocity profile with the non-constant high viscosity layer clearly showed the difference from the case of constant viscosity for λ_D = 2 and 5 nm. This result implies that the difference becomes the largest when the EDL thickness is comparable with the non-constant viscosity layer and that the high concentration of ions in the EDL causes to increase the viscosity. The relationship between the high concentration in the EDL and the viscosity gradient has to be investigated in more detail from the viewpoint of molecular dynamics simulations in the future.

Results of the LD simulations with the non-constant viscosity layer

In the main text, we have carried out the simulation of ssDNA transport in the nanochannel in the presence of the non-constant viscosity layer. For the reference, the analysis of ssDNA mobility and deformation in the nanochannel with the non-constant viscosity layer is presented in Figs. S3-S7, corresponding to Figs. 2, 4-7 in the main text, respectively.

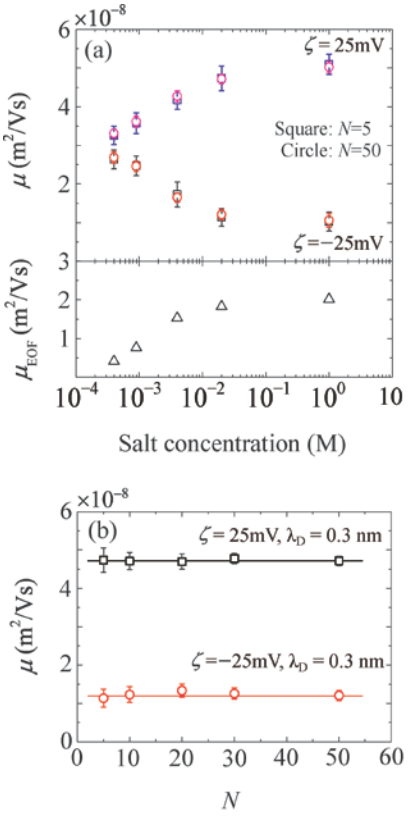

FIGURE S3. The electrophoretic mobility, μ, of ssDNA with non-constant viscosity layer, corresponding to the computational conditions of Fig. 2 in the main text.

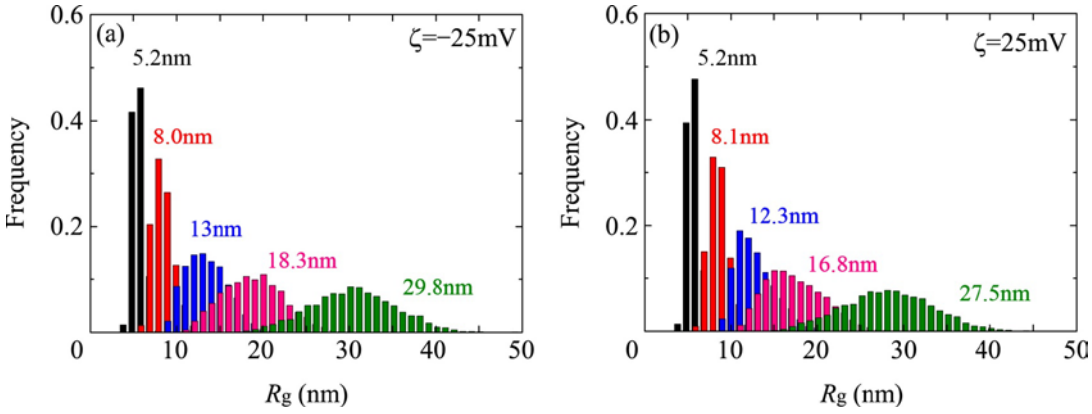

FIGURE S4. Distributions of R_g in the nanochannel for the variety of N resulting from (a) ζ = −25 mV and (b) ζ = 25 mV in the presence of non-constant viscosity layer, corresponding to Fig. 4 in the main text. Mean values of R_g in the case of N = 50 are 29.8 and 27.5 nm for ζ = −25 and 25 mV, respectively. Legend: black, N = 5; red, N = 10; blue, N = 20; pink, N =30; green, N = 50.

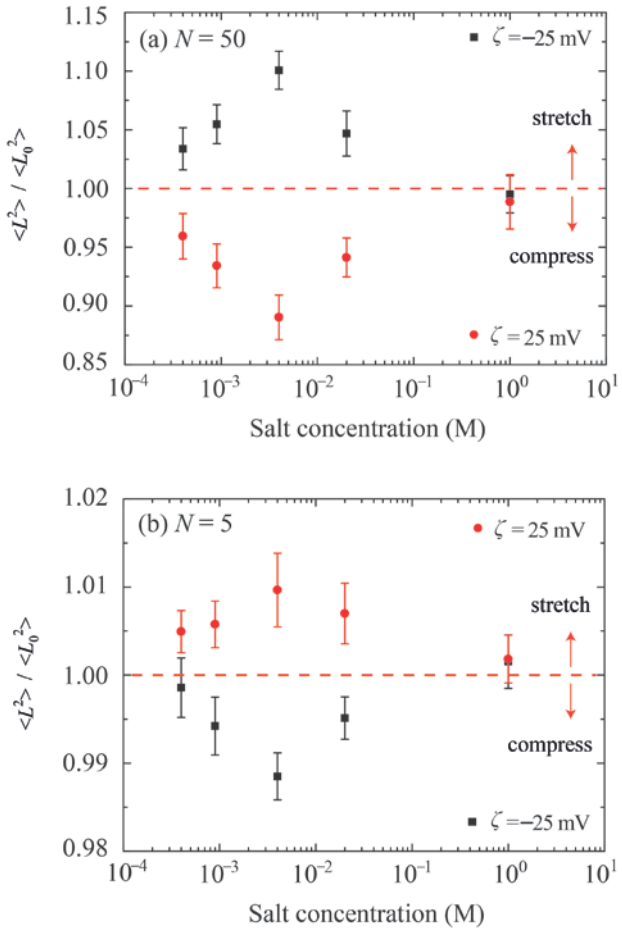

FIGURE S5. Mean square end-to-end distances, $\langle L^2 \rangle$, of ssDNA exposed to E_r in a nanochannel at various values of ζ potential and λ_D in the presence of non-constant viscosity layer, for comparison with Fig. 5 in the main text. Data are shown for the polymer lengths (a) N = 50 and (b) 5.

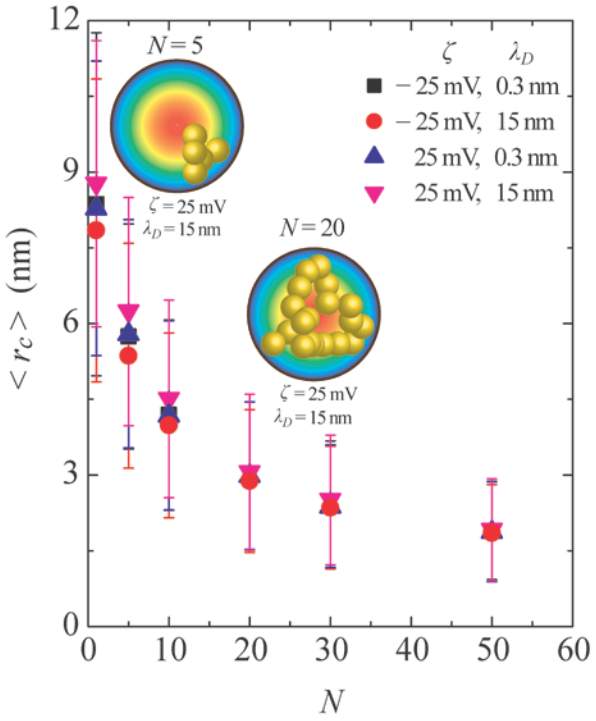

FIGURE S6. Ensemble average of the mass-center radial position, $\langle r_c \rangle$, as a function of the polymer length, N, in the presence of non-constant viscosity layer, for comparison with Fig. 6 in the main text. Legend: ζ = –25 mV, λ_D = 0.3 nm (black squares); ζ = –25 mV, λ_D = 15 nm (red circles); ζ = 25 mV, λ_D = 0.3 nm (blue triangles); and ζ = 25 mV, λ_D = 15 nm (pink inverted triangles). The error bars that represent the standard deviations reflect the Brownian motion of ssDNA inside the nanochannel.

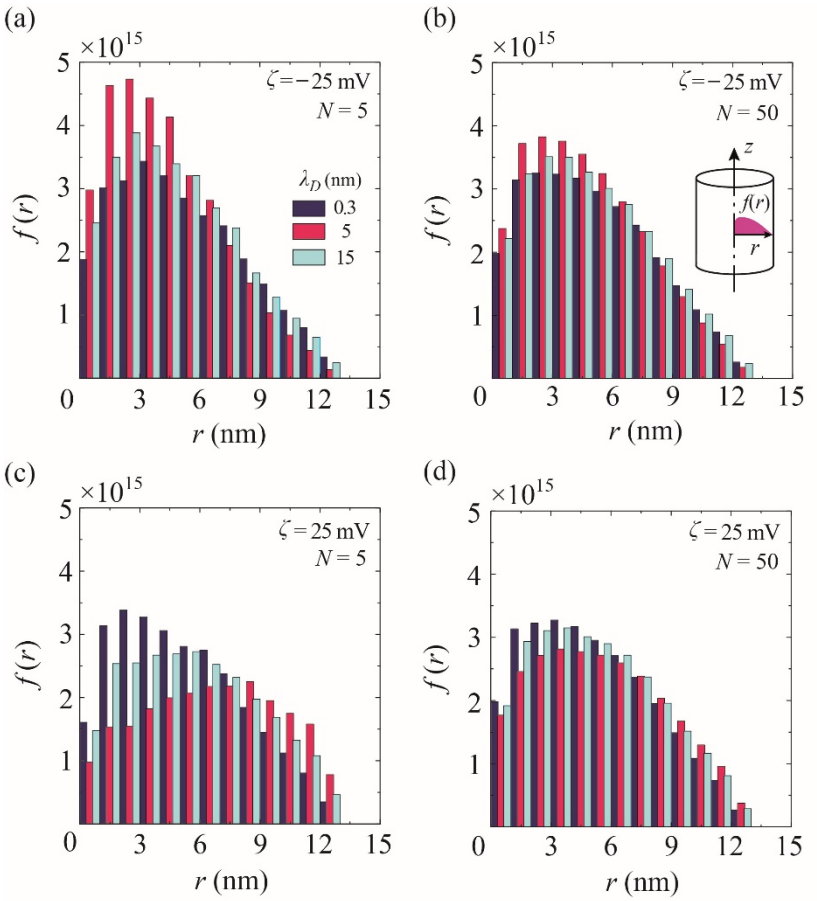

FIGURE S7. Discretized distribution function, $f(r)$, of the radial position of individual coarse-grained beads in a channel with the non-constant viscosity layer, for comparison with Fig. 7 in the main text. Legend: (a and b) a negative ζ potential of −25 mV and polymer lengths of (a) N = 5 and (b) 50, and for (c and d) a positive ζ potential of 25 mV and (c) N = 5 and (d) 50. The radial position of each molecule was sampled at 10 μs intervals over the last 1.0 ms of simulation time.

References

1. Qian, W. X., K. Doi, …, S. Kawano, 2014. Theoretical study of the transpore velocity control of single-stranded DNA. *Int. J. Mol. Sci*. 15:13817–13832.
2. Nagahiro, S., S. Kawano, and H. Kotera. 2007. Separation of long DNA chains using a nonuniform electric field: A numerical study. *Phys. Rev. E*. 75:011902.
3. Doi, K., T. Haga, …, S. Kawano. 2010. Development of coarse-graining DNA models for single-nucleotide resolution analysis. *Philos. Trans. R. Soc. A* 368:2615–2628.
4. Tinland, B., A. Pluen, …, G. Weill. 1997. Persistence length of single-stranded DNA. *Macromol. Macromolecules*. 30:5763–5765.
5. Stellwagen, E., Y. Lu, and N. C. Stellwagen. 2003. Unified Description of Electrophoresis and Diffusion for DNA and Other Polyions. *Biochemistry.* 42:11745–11750.
6. Wang, Y., P. Keblinski, and Z. Chen. 2012. Viscosity calculation of a nanoparticle suspension confined in nanochannels. *Phys. Rev. E*. 86:036313.
7. Levine, S., J. R. Marriott, …, N. Epstein, 1975. Theory of electrokinetic flow in the cylindrical capillaries at high zeta-potentials. *J. Colloid Interface Sci*. 52(1):136–149.
8. Rice, C. L., and R. Whitehead. 1965. Electrokinetic Flow in a Narrow Cylindrical Capillary. *J. Phys. Chem*. 69:4017–4024.
9. Abramowitz, M., and I. Stegun. 1972. A. Handbook of Mathematical Functions with Formulas, Graphs, and Mathematical Tables, Dover Publications, New York.
10. Zhang, J. F., B. D. Todd, and K. P. Travis. 2004. Viscosity of confined inhomogeneous nonequilibrium fluids. *J. Chem. Phys*. 121:10778.